HHS Public Access

Author manuscript

IEEE Trans Biomed Eng. Author manuscript; available in PMC 2022 September 01.

Published in final edited form as:

IEEE Trans Biomed Eng. 2021 September ; 68(9): 2615–2625. doi:10.1109/TBME.2020.3037820.

Inertial Sensor Algorithms to Characterize Turning in Neurological Patients with Turn Hesitations

Vrutangkumar V. Shah[*],
Oregon Health & Science University, Portland, OR, USA

Carolin Curtze,
University of Nebraska at Omaha, Omaha, NE, USA

Martina Mancini [Member IEEE],
Oregon Health & Science University, Portland, OR, USA

Patricia Carlson-Kuhta,
Oregon Health & Science University, Portland, OR, USA

John G. Nutt,
Oregon Health & Science University, Portland, OR, USA

Christopher M. Gomez,
The University of Chicago, Chicago, IL, USA

Mahmoud El-Gohary,
APDM, Inc, Portland, OR, USA

Fay B. Horak,
Oregon Health & Science University, Portland, OR, USA; APDM, Inc, Portland, OR, USA

James McNames [Senior Member, IEEE]
Department of Electrical and Computer Engineering, Portland State University, Portland, OR, USA; APDM, Inc, Portland, OR, USA

Abstract

Background.—One difficulty in turning algorithm design for inertial sensors is detecting two discrete turns in the same direction, close in time. A second difficulty is underestimation of turn angle due to short-duration hesitations by people with neurological disorders. We aim to validate and determine the generalizability of a: I. Discrete Turn Algorithm for variable and sequential turns close in time and II: Merged Turn Algorithm for a single turn angle in the presence of hesitations.

[*]Vrutangkumar V. Shah (shahvr@ohsu.edu).

Dr. El-Gohary, Horak, and McNames have a significant financial interest in APDM, a company that may have a commercial interest in the results of this research and technology. These potential individual conflicts have been reviewed and managed by OHSU.

Methods: We validated the Discrete Turn Algorithm with motion capture in healthy controls (HC, n=10) performing a spectrum of turn angles. Subsequently, the generalizability of the Discrete Turn Algorithm and associated, Merged Turn Algorithm were tested in people with Parkinson's disease (PD, n =124), spinocerebellar ataxia (SCA, n=51), and HC (n=125).

Results: The Discrete Turn Algorithm shows improved agreement with optical motion capture and with known turn angles, compared to our previous algorithm by El-Gohary et al. The Merged Turn algorithm that merges consecutive turns in the same direction with short hesitations resulted in turn angle estimates closer to a fixed 180-degree turn angle in the PD, SCA, and HC subjects compared to our previous turn algorithm. Additional metrics were proposed to capture turn hesitations in PD and SCA.

Conclusion: The Discrete Turn Algorithm may be particularly useful to characterize turns when the turn angle is unknown, i.e. during free-living conditions. The Merged Turn algorithm is recommended for clinical tasks in which the single-turn angle is known, especially for patients who hesitate while turning.

Keywords

Turning; inertial sensors; mobility; Parkinson's disease (PD); Spinocerebellar ataxia (SCA); healthy controls (HC)

I. Introduction

Turning is ubiquitous and complex during daily activities as it requires the central nervous system to reorient the body segments towards a new direction while continuing with the ongoing step cycle and maintaining postural stability [1]. However, defining the start and end of a turn in order to characterize the quality of turning with wearable sensors is difficult because of the smooth transitions between straight walking periods that naturally involve rhythmic trunk and leg yaw rotations and body segment rotations involved in turning [2–4]. A common problem is delay in detecting the start of a turn and anticipatory detection of end of a turn, resulting in underestimation of turn angle [2], [3]. In addition, brief hesitations during a turn, which are very common in people with neurological disorders [5], make it particularly challenging to define the start and end of each turn.

Wearable inertial sensors have been used to characterize turning in the laboratory during standard clinical tasks involving a fixed turn angle (such as 180° for a Timed Up and Go Test (TUG)) [1], [3], [4], [6–19]. More recently, turns have been characterized in the laboratory, and in the community setting [1–4], [6–19]. Researchers have proposed a variety of definitions to identify a turn depending on the location of sensors and signal processing approach but very few have validated the accuracy of measuring turn angle (see the summary table in Appendix for more details).

Many studies used statistical characteristics of spatiotemporal gait parameters to define a turn. For example, Mariani et al. [4] used feet sensors and defined a turn as strides with foot turning angles larger than 20°. The accuracy and precision of their turn algorithm against optical motion capture systems were 1.6 ± 6.1° for 180° turns. In a subsequent paper, Mariani et al. [20] tested the turn algorithm from feet sensors in people with PD (ON

and OFF states) and HC, and reported 0.12 ± 3.59° as accuracy and precision of their turn algorithm against optical motion capture systems.

A recent turning algorithm from our group, El-Gohary et al. [1], used a threshold on the rotational rate of the lumbar sensor. Specifically, a candidate turn was defined as a trunk rotation around the vertical plane with a minimum of 40°/sec, and a onset and end of the turn was defined with a threshold of 15°/sec. The algorithm was validated in the laboratory against optical motion capture and video analysis. Compared to optical motion capture and video, the algorithm reported a sensitivity of 0.90 and 0.76 and a specificity of 0.75 and 0.65, respectively, although the turn angle accuracy was not reported. Later, Novak et al. [17] proposed to combine orientation and angular velocity from the lumbar sensor for better turn onset detection. In addition, they investigated the effect of sensor locations (head, upper back, lower back, thigh, shank, and foot) on turn algorithm performance and found that inertial sensors should be placed on the trunk (either sternum or lumbar spine) rather than the legs or feet for most accurate turn onset detection. Similarly, Ortega-Bastidas et al. [11] used an orientation angle from a lumbar sensor to detect turns and validated turn duration against visual observation from a video. Both Novak et al. [17] and Ortega-Bastidas et al. [11] did not provide the accuracy of the turn angle. Note that the validation of the start and end time of a turn against motion capture system/video analysis does not guarantee a very good or excellent turn angle accuracy. For example, recently Rehman et al. [12] showed an excellent agreement between video rater and motion capture system for start and end of a turn (ICC ≥0.99), but the reported turn angles were 172.59 ± 22.99° (for controls) and 168.37 ± 29.33° (for PD) against the known 180-degree turn.

All of the above proposed turning algorithms were validated in laboratory settings where the turn angle was predefined. To overcome this limitation and to determine the accuracy of the turning algorithm in free-living condition, recently, Pham et al. [2] used a lumbar-placed gyroscope and accelerometer for attitude estimation and used angular displacement around z-axis to define a start and end of a turn in PD with 90 minutes of free-living activities. In addition, they defined turn hesitations as a movement with a duration of less than 0.5 s and a magnitude less than 10% of the magnitude of the previous and following turns (each must be greater than 10° and have the same direction). If two turns were separated by such a hesitation, they were merged and defined as one single turn. The algorithm was validated against video recording observations, and the reported turn angle accuracy was 0.06 ± 014° (mean error ± SEM), where turn angle error is the difference in turning angle from video observers and the algorithm. However, we recommend caution about interpreting these results as it is hard to estimate turn angle accurately just by looking at video recordings. Later, the same group reported turn angles of 177±8° against known turn angles of 180° [8].

In summary, all of the published turn algorithms validated and tested their success either with participants from one particular neurological disorder/only from healthy adults, or single protocol with limited sample sizes (see the summary table in Appendix for more details) [1–4], [6–19]. Furthermore, only a handful of researchers have shown the accuracy of turn angle estimation against either optical motion capture systems/video analysis or a known angle using their proposed algorithms for standard clinical tasks. As a result, it is difficult to test the generalizability of published turn algorithms across patient cohorts. All

measures characterizing a turn, such as turn velocity and duration, are based on the correct detection of the start and end of a turn. Although there is no accepted definition of the start and end of a turn, making sure that the resultant turn angle estimation is close to an expected turn angle gives us confidence about the performance of an algorithm. Hence, in this study, we used optical motion capture system and/or known turn angles as validation tools for measuring turn angles with the proposed turning algorithms in people with a variety of neurological disorders, as well as neurotypical adults.

This manuscript presents two new algorithms for quantifying turn angle with inertial sensors. The objectives are to validate and determine the generalizability of a: I. Discrete Turn Algorithm for sequential turns close in time (with variable turn angles) and II: Merged Turn Algorithm for detecting a single known turn angle, even with hesitations due to neurological disorders. For aim I, we validated the Discrete Turn Algorithm against optical motion capture system in a spectrum of turn angles (45°, 90°, 145°, and 180° turns) in 10 healthy control (HC) subjects. Next, we tested the generalizability of the Discrete Turn Algorithm with a sequence of known turn angles (90°and 180° turns) in 124 people with Parkinson's disease (PD) and 64 subjects. For aim II, we validated the Merged Turn Algorithm against a single known turn angle (180° turns) in the same cohorts as no. 1 (but with 2-minute walk protocol), 51 people with spinocerebellar ataxia (SCA) and 50 HC with similar age as that of SCA with 2-minute walk test. Next, we test the generalizability of the Merged Turn Algorithm in 125 HC with a single know turn angle of 180° in 400m fast walk test. To test the performance of the proposed turning algorithms with the state-of-art turning algorithm, we additionally compared the results of the Discrete Turn and Merged Turn Algorithms with our previous turning algorithm by El-Gohary et al. [1]. The details of the five datasets are described in Table II. The five datasets were needed to capture the turn hesitation in patients with neurological disorders and to determine generalizability across various cohorts and protocols.

We compare our new algorithms with the algorithm by El-Gohary et al. [1] because this commercially available system has been validated, and it was readily available to us in a reproducible form. The El-Gohary algorithm used a single smoothing filter for both turn detection and to determine a start and end of a turn. It also only used a single sensor (lumbar) for the turn detection algorithm. In contrast, the proposed Discrete Turn Algorithm uses two thresholds and two different filters, one for turn detection and the other to determine a start and end of a turn. Further, the Discrete Turn Algorithm averages the vertical rotational rates from all sensors (lumbar and sternum) placed on the trunk. The Merged Turn Algorithm provides unique steps to merge nearby turns detected by the Discrete Turn Algorithm in case of hesitations.

The remainder of this paper is organized as follows. Section II describes the two proposed algorithms (Discrete Turn Algorithm and Merged Turn Algorithm). Section III describes the protocol and results of the Discrete Turn Algorithm, and Section IV describes the protocol and results of the Merged Turn Algorithm. Section V presents the discussion, and finally we conclude the paper in Section VI.

II. Algorithm Design

The flowchart of the two algorithms is shown in Fig. 1. Any medical-grade inertial sensors containing an accelerometer, gyroscope, and magnetometer can be used to quantify a turn using the proposed turn algorithms described in this section. Both of the proposed turning algorithms require synchronized sensors to be placed on the lumbar or/and sternum for yaw turn estimation to quantify a turn. Sensors on the feet were used for step detection only.

1. Discrete Turn Algorithm

Step 1: Yaw turn estimation: Most companies that manufacture and produce inertial sensors include a proprietary algorithm for estimating the orientation of the sensor relative to an Earth reference frame, which uses the gravitational force detected by the accelerometers as the vertical axis and the magnetic field as a heading reference. These algorithms fuse the information from accelerometers, gyroscopes, and magnetometers to estimate the orientation of the sensor as accurately as possible. This type of algorithm is often called an attitude and heading reference system (AHRS). The principles underlying these algorithms are well known [1], [21], [22]. Typically these use the gravitational component of the accelerometers to serve as the vertical reference and the magnetometers as a heading reference. Our turn algorithm uses the orientation provided by an AHRS algorithm to rotate the triaxial gyroscope signals from a subject reference frame into an Earth reference frame. Of these signals, we only retain the rotational rate about a vertical axis pointed upwards. This does not require a heading reference, so this approach can be used even if a magnetometer is not available.

Typically, the rotational rate will include a gradual and temporary increase in the magnitude of the rotational rate due to the turn. However, it will also typically include other fluctuations due to other movements of the subject, such as axial rotations that normally occur as part of the gait cycle. In some subject populations, there may also be atypical movements due to tremor, dyskinesia, or ataxia. To better isolate the rotational rate due to the turn, we lowpass filter the signal with a finite impulse response (FIR) filter. We have chosen an impulse response that is symmetric, weighted moving average with an impulse shape that is an Epanechnikov kernel [23],

$$h[n] = \begin{cases} 1 - \left(\frac{n}{M}\right)^2, & |n| \leq M \\ 0 \quad , & |n| > M \end{cases}$$

where $h[n]$ is the impulse response of the filter, M is the half-width of the filter, and n is the discrete-time index. The filter design has a symmetric impulse response and is in the same class of filters as moving averages, but this uses a weighted moving average where the weight is concentrated near the center of the window for better time resolution for the same amount of smoothing. We chose this impulse response because it is easy to implement, it is optimal in a mean square sense for a related application of density estimation, and it is non-negative [23]. Other non-negative kernels could have been used and would have produced a similar performance. We chose a non-negative impulse response instead of a frequency-selective lowpass filter because the purpose of this filter was to smooth the signal

with a weighted local average, rather than to eliminate specific frequencies. Additionally, most frequency-selective filters have an impulse response with ripples that can make it more difficult to determine the edges corresponding to the start and end of a turn than smoothing filters with non-negative impulse responses.

This filter is completely specified by the half-width M, which determines the amount of smoothing. The smoothing should be sufficient to eliminate high-frequency axial movements that are not associated with turns, but it should not be so smooth that it attenuates the amplitude of the turn and makes detection more difficult. The gait cycle typically has a duration of approximately 1 s [24], [25], and turn durations are typically around 2–5 s in duration [15], [16], [26]. We chose an M such that the impulse response duration was $d_d = 1.476$ s, and the filter had a cutoff frequency of 0.8 Hz.

If multiple sensors at different locations on the body are used simultaneously, this process of estimating the rotational rate about the vertical axis can be used for each sensor separately. If the signals from the sensors are synchronized in time, the vertical rotational rates can be combined by calculating the average. However, different parts of the body may initiate and complete the turn at different points in time. For example, the wrist may begin to rotate before the trunk.

Fig. 2 shows an example of the vertical rotational rates calculated from synchronous sensors worn at four different locations on the body. The smoothed signal used for turn detection is also shown by the thick dark lines in each plot. This figure illustrates that large-amplitude high-frequency movement associated with the gait cycle shown for the sensor on the left foot and right wrist. The effects of the gait cycle are also present, but at a reduced amplitude in the plots for the lumbar and sternum.

We are primarily interested in how the trunk of the body turns. When we have multiple sensors on the trunk, such as both the lumbar and the sternum, we combine the rotational rates of these sensors to help reduce the noise due to other movements at each sensor location. The sensors on the feet are only used for step detection to determine how many steps were taken during each turn.

Step 2: Calculate Absolute Smoothed Rotational Rate.—Calculate the smoothed vertical rotational rate with the detection filter and take the absolute value. This results in a signal that contains a smoothed increase that does not depend on the direction of the turn.

Step 3: Find Valid Minima.—To ensure the algorithm does not include shallow, local minima that may result from a brief slowing or hesitations during a turn, we only retain minima that are at least some amount, *eta*, below candidate maxima. We only consider maxima that are above our velocity threshold and may represent turns. Fig. 3 shows an example of minima that meet our validation criteria (dots) and minima that do not meet the criteria (x's).

Step 4: Verify Maxima is Sufficiently Large.—Detect the maximum between each pair of adjacent minima. If the maximum is above a turn velocity threshold ν_d, declare the period

between the minima as a detected turn. The horizontal line in Fig. 3 shows this threshold as a horizontal line clearly indicating the detection of a turn.

Step 5. Find Turn Start and End.—The smoothing used to detect the turn smooths the signal too much to determine the edges that demarcate the start and end of a turn. Turns can begin and end abruptly, relative to the duration of the turn. To account for this we apply a second smoothing filter to the vertical rotational rate and calculate the absolute value. We chose the M for this filter such that the impulse response duration for this edge filter was 0.383 s and the cutoff frequency was 3.0 Hz. This was a balance between the tradeoffs of smoothing too much, which would cause the turn duration to be overestimated, and not smoothing enough, in which case a brief slowing or pause during a turn might falsely be detected as the end of a turn. The edges are declared as the first time to the left and right of the maxima identified in Step 4 that the second smoothing filter drops below the edge threshold ν_e. This is illustrated in Fig. 4.

Step 6. Eliminate Small Turns.—Once the edges of a potential turn are detected, the turn angle can be estimated by numerical integration of the vertical rotational rate. The final step of the algorithm eliminates turns with turn angles that are less than a threshold of $\theta =$ 40°. Turns with angles less than this amount would typically not be judged as a complete turn in clinical studies, and might comprise curved walking rather than a turn.

Table I lists all of the design parameters and the values we chose to obtain the most accurate detection on our data sets.

Fig. 5 shows an example of the same turn as detected the El-Gohary algorithm [1] and the Discrete Turn Algorithm. This figure shows many of the advantages and rationale for the design of the new algorithm. The El-Gohary algorithm used a single threshold and smoothing filter for both detection and edge detection. It also only used a single sensor for detection, rather than averaging the vertical rotational rates from all sensors placed on the trunk. These limitations caused the algorithm to significantly under-estimate the duration of the turn angle.

2. Merged Turn Algorithm

If the recording is obtained during a protocol in which the subject is known to perform a specific, fixed turn angle such as 180° with walking in between, three further processing steps are used after the Discrete Turn Algorithm to more accurately detect and estimate the turn properties. Some neurological diseases and other conditions that affect turning often cause subjects to slow, halt, or hesitate during a turn. The turn algorithm described in Steps 1-6 may identify or detect these as several separate turns that occur close together in time as the subject attempts to turn 180°. The Merged Turn Algorithm described in this section may merge separate turns detected by the Discrete Turn Algorithm into a single turn if the combined turns are closer to the expected turn angle.

Step 7. Merge Close Turns.—This merging step identifies all of the cases where one turn ends, and another begins in a period less than some specified interval, t_s, and where the

turn angle of the merged turns would be closer to the fixed, prescribed turn angle than the turn angle would be if the turns were not merged.

Step 8. Expand or Contract Turn Start and End.—This step provides a further adjustment of the turn edges to attain a turn with an angle closer to the fixed turn angle. Rather than using a single threshold as in Step 5, this step allows the turn to be expanded so long as the smoothed vertical rotation rate is above an expansion threshold ν_x and such an expansion would bring the turn angle closer to the fixed turn angle. Similarly, a turn can be contracted so long as the smoothed vertical rotation rate is below a contraction threshold ν_c and such a contraction would bring the turn angle closer to the fixed turn angle. At each increment of expansion or contraction, the algorithm selects the edge at the start or end of the turn based on which will move the turn angle the closest to the fixed turn angle.

3. Turn Characterization:

Once a turn is detected (either using the Discrete Turn or the Merged Turn Algorithm), we used a step detection algorithm from feet sensors [27], along with the turn detection from sternum/lumbar to characterize the quality of the turn. We implemented the algorithms in C++, but they could be implemented in any modern programming language from the description in this paper. The algorithms use non-causal processing steps and thereby can only be applied after the recordings are completed. They cannot be directly implemented for real-time turn detection, though it is possible to implement them so they detect turns with a small lag. We calculated the following metrics to quantify the most important properties of turns:

Turn Duration.—Duration of the turn defined as the time elapsed between the start and the end of the turn.

Turn Angle.—Total change in heading angle of the turn calculated as the difference between the ending and starting heading angle.

Steps in Turn.—A total number of steps detected during the turn.

Turn Rate Average.—Average of the vertical rotational rate during the turn period.

Turn Rate Maximum.—The maximum rate of the vertical rotational rate during the turn period.

Turn Hesitations.—The number of times a subject hesitates > t_s during the prescribed turn is also recorded for each turn (only for Merged Turn Algorithm).

III. Protocols And Results Of Discrete Turn Algorithm For Sequential Turns

Table II provides a summary of the studies and protocols used to test the performance and generalizability of the two proposed turning algorithms. In this section, we describe the studies and protocols used to test the performance of the Discrete Turn Algorithm and provided the results.

Overview.

To demonstrate the generalizability of our Discrete Turn Algorithm for sequential variable turns, we have used two datasets (*Validation and Walk-through doorway studies*). The *Validation study* included a set of healthy subjects performing a series of turns at a normal and fast speed, in the center of an optical motion capture space, and used for validation against motion capture system. The *Walk-through doorway study* included participants from the PD/HC study performing 3 turns during a walk through a doorway, and used to test the generalizability of the Discrete Turn Algorithm.

Common protocol for all studies.

The subjects wore 6 inertial sensors (opals by APDM Wearable Technologies, Portland, oR, usA) that included triaxial accelerometers, gyroscopes, and magnetometers sampled at 128 Hz. The opal is light weight (22 g), has a battery life of 16 h, and includes 8 GB of storage. The sensors were attached to both feet, wrists, the sternum, and lumbar regions. We used only feet, sternum, and lumbar sensor data in this analysis.

Exclusion criteria for all the subjects were an inability to follow instructions and other factors affecting gait such as hip replacement, musculoskeletal disorders, uncorrected vision or vestibular problems, or inability to stand or walk in the home without an assistive device. The experimental protocols for PD and HC, normative, and optical motion capture validation datasets were approved the Joint Institutional Review Boards of Oregon Health & Science University and the VA Portland Healthcare System. The SCA and HC dataset was approved by the Institutional Review Board of The University of Chicago. All the subjects provided informed written consent.

Protocols

Validation Study Protocol: Ten healthy older adults (age: 72 ± 5.8 years old) were recruited for this study [28]. Subjects performed pre-planned turns to the left and right in the middle of a 2.5 m radius circle, at different turn angles (45°, 90°, 135°, and 180°) while walking at normal and fast speeds [28]. Floor markings similar to a clock face consisting of a turning point in the center and turn angle marks in the periphery (2.5 m radius circle) were used as guidance to indicate turn angle. Subjects were instructed to pass through the origin of the circle and walk towards a specified mark in the periphery. Concurrently with wearing inertial sensors (Opals by APDM), optical motion capture data were collected at 120 Hz (Raptor-H (8) and Osprey (4) cameras by Motion Analysis Inc., Santa Rosa, CA). All subjects were outfitted with 30 retroreflective markers in a modified Helen Hayes marker set configuration. Markers were placed on the head (front, back, and lateral), thorax and arms (acromion, sternum, offset, lateral epicondyle of humerus, and distal radius), pelvis (sacrum, anterior superior iliac spine (ASIS)), legs (thigh, lateral epicondyle of the femur, shank, lateral and medial malleolus), and feet (1st and 5th metatarsal head, and posterior calcaneus).

Turn Angle Estimation using Motion Capture for Validation Study: The optical motion capture data was used to calculate the turn angle. All 30 markers were tracked, and gaps were filled using spline interpolation. The marker data were low-pass filtered

using a 4th order phaseless 6 Hz Butterworth filter. The instantaneous position of the whole-body center of mass (CoM) was estimated as the weighted average of 15 segments using kinematic data and anthropometric tables [29]. From the path-of-progression of the whole-body CoM, we calculated the instantaneous heading. The turn angle was defined as the total change in heading angle when passing through the optical motion capture volume, i.e., within a 1.25 m radius circle from the origin.

Walk-through doorway Study Protocol: The *Walk-through doorway study* included participants from the PD/HC study performing 3 turns during a walk through a doorway. Subjects were asked to make one 90° turn just after exiting the doorway, followed by 2-3 steps and a 180° turn, a few more steps, another 90° turn, and return through the doorway. The subjects performed walk-through doorways task with and without a dual-task, and a subset of PD subjects came for multiple visits as a part of the Agility Boot Camp study [30] resulting in 796 trials.

PD/HC Study: One hundred twenty-seven subjects with mild to moderate PD (age: 69.20 ± 7.71 years, UPDRS part III total tested *OFF* medication: 40.56 ± 12.77), 64 age-matched healthy control subjects (HC) (age: 67.36 ± 8.21 years) participated in the study. Inclusion criteria for PD were (a) age between 50–90 years old, (b) no major musculoskeletal or peripheral disorders (other than PD) that could significantly affect their balance and gait, (c) ability to stand and walk unassisted and d) diagnosis of idiopathic Parkinson's disease treated with levodopa by a movement disorders specialist. People with PD were further divided into the freezer (FOG) and non-freezer (nFOG) based on the new freezing of gait questionnaire [31].

Statistical analysis.—Turn angle agreement between motion capture and an inertial sensor algorithm was assessed using the Bland and Altman method [32], and intraclass correlation coefficient (ICC), specifically ICC (2,1) [33]. All statistical analysis was performed using R Version 1.1.456 software.

Results

Validation Study Results: *The* Discrete Turn Algorithm showed improved agreement with the motion capture system compared to the algorithm by El-Gohary et al. [1] on the validation dataset. Specifically, the histogram of turn angle estimates is in close agreement with the motion capture estimates using the Discrete Turn Algorithm compared to the El-Gohary et al. [1] (see Fig. 6). Further, bias was lower in the Discrete Turn Algorithm (−0.386 [−1.19—0.413]) compared to El-Gohary et al. [1] (0.833 [−0.43—2.11]) (see Fig. 7). The limits of agreement were narrower for the Discrete Turn Algorithm, indicating improved agreement. The lower and upper bounds of the limit of agreement (LOA) was smaller in Discrete Turn Algorithm (Lower LOA:−15.75 [−17.13— −14.391], and Upper LOA: 14.986 [13.620—16.354]) compared to El-Gohary et al. [1] (Lower LOA: −22.013 [−24.196— −19.83], and Upper LOA: 23.678 [−21.495—25.860]). In addition, the intraclass correlation coefficient was higher for Discrete Turn Algorithm ($ICC_{2,1}$=0.989 [0.986-0.991]) compared to El-Gohary et al. [1] ($ICC_{2,1}$=0.970 [0.963–0.976]).

Walk-through Doorway Study Results: The histogram of turn angle estimates was tighter using the Discrete Turn Algorithm compared to the algorithm of El-Gohary et al. [1] (see Fig. 8) when applied to **walk-through doorways** dataset (total turns n = 2959). In addition, we observed a reduction in turn angle estimates of 270° (Fig. 8, inset) compared to El-Gohary et al. [1] confirming that the Discrete Turn Algorithm was able to separate nearby turns (90° and 180° successively or vice versa), which is considered as a single turn in the El-Gohary algorithm [1].

IV. Protocols and Results of Merged Turn Algorithm for a Single Fixed Turn

Overview.

To check the generalizability of our proposed Merged Turn Algorithm, we have used datasets from 3 studies in our laboratory involving a single fixed turn angle. Specifically, for the algorithm tuning process, we have datasets from 2 cohorts of neurological patients with their age-matched healthy controls (*PD/HC and SCA/HC studies*) performing 180° turns during the 2-minute walk test. We selected studies with PD and SCA neurological disorders because both likely include slow turns with hesitations during the turns due to freezing and/or imbalance, respectively. To test the performance of the Merged Turn Algorithm, we have an independent test dataset with healthy control subjects (*Normative study*) performing a fast 2-minute walk test. We have selected a fast walk to investigate the performance of the proposed turn algorithm across a range of walking speed.

Protocols

PD/HC Study Protocol: All subjects from PD/HC study were asked to perform a 2-min walk test (subjects were instructed to walk at a comfortable pace back and forth continuously between two lines on the floor 7.5 m apart for 2 min).

SCA/HC Study Protocol: Fifty-one people with SCA (age: 54.51 ± 13.31 years, SARA score: 10.85 ± 4.31) and 50 age-matched healthy control subjects (HC) (age: 55.78 ± 14.77 years) participated in the study. Inclusion criteria for SCA were (a) age between 18–75 years old, (b) no major musculoskeletal or peripheral disorders that could significantly affect their balance and gait, (c) ability to stand and walk unassisted, and d) a clinical diagnosis of SCA by a movement disorders specialist, and stand or walk unassisted for 30 sec. All subjects were asked to perform a 2-min walk test (subjects were instructed to walk at a comfortable pace back and forth continuously between two lines on the floor 7.5 m apart for 2 min).

Normative Study Protocol: One-hundred twenty-five healthy control subjects (age range: 19 – 88 years old) participated in the study. Inclusion criteria for normative were a) no walking aides, b) no neurological conditions, c) no musculoskeletal conditions affecting gait, d) no joint replacement within the past year, e) no pain affecting gait, f) no falls in the past year, g) dementia. Cones were placed on the floor 20 m apart, and subjects were asked to walk ten laps as fast as possible, making clockwise turns around the cones.

Statistical analysis.—To investigate the performance of the proposed turning algorithm compared to the turning algorithm by El-Gohary et al. [1], we computed the receiver-operator characteristic (ROC) area under the curve (AUC) [34].

Correlation between various turn metrics and age was calculated using Pearson's correlation. All statistical analysis was performed using R Version 1.1.456 software.

Results

PD/HC and SCA/HC Study Results: The algorithm by El-Gohary et al. [1] often resulted in several small turns during 180° turns during the 2-minute walk test, especially in people with PD or SCA. Figure 9A illustrates yaw angular rotation of the pelvis (top) during three, 180° turns that the original algorithm detected as one to three smaller turns (bottom). In contrast to the El-Gohary et al. [1], our new, Merged Turn Algorithm correctly combines small turns that occur very close in time in the same direction, and single 180° turns with multiple hesitations (Fig. 9B).

The Merged Turn Algorithm resulted in narrower group dispersion of the group frequency distribution histograms of turn angle estimates, and the group means of turn angle are closer to 180° compared to the El-Gohary algorithm. Figure 10A shows how both the PD subjects, and especially PD with FOG, show turns that are smaller than 180°, unlike age-matched controls using the El-Gohary algorithm [1] (mean and SD turn angle: 170.51 ± 12.72°). Figure 10B shows that the new Merged Turn Algorithm resulted in turn angles closer to 180° for the PD group (176.63 ± 6.42°). Figure 11A shows the large underestimation of 180° turns in the SCA group using the El-Gohary algorithm [1] (160.52 ± 33.14°). In contrast. Fig. 11B shows an improved estimation of 180° turn angles in SCA subjects, who have many hesitations during turning, using the Merged Turn Algorithm (175.99 ± 11.87°).

As a result of turn angle estimates closer to 180° using the Merged Turn Algorithm, AUC to separate turning characteristics between neurological and age-matched cohorts have increased for both groups. Specifically, the AUC for the turn duration and the number of steps required to complete a turn for PD/HC has increased to 0.91 and 0.87, compared to El-Gohary et al. [1], which were 0.87, and 0.80, respectively (see Table III). Similarly, the AUC for the turn duration and the number of steps required to complete a turn for SCA/HC has increased to 0.84 and 0.87, compared to El-Gohary et al. [1], which were 0.76, and 0.68, respectively (see Table IV).

The Merged Turn Algorithm provides a new turning characteristic, the number of hesitations. We found that 6 % of people with PD (10.53% FOG, and 2.86% nFOG) hesitated during their 180° turns with an average number of hesitations equal to 0.12 ± 0.62 (minimum: 0, and maximum: 6) across an average of 10.48 ± 2.94 turns per trial (see Fig. 12A). Similarly, 25% of people with SCA hesitated during their 180° turns with an average number of hesitations equal to 0.98 ± 2.24 (minimum: 0, and maximum: 10) across an average of 7.92 ± 3.14 turns per trial (see Fig. 12B). None of the healthy control subjects showed hesitations during a turn.

The Merged Turn Algorithm provides a new turning characteristic, the number of hesitations. We found that 6 % of people with PD (10.53% FOG, and 2.86% nFOG) hesitated during their 180° turns with an average number of hesitations equal to 0.12 ± 0.62 (minimum: 0, and maximum: 6) across an average of 10.48 ± 2.94 turns per trial (see Fig. 12A). Similarly, 25% of people with SCA hesitated during their 180° turns with an average number of hesitations equal to 0.98 ± 2.24 (minimum: 0, and maximum: 10) across an average of 7.92 ± 3.14 turns per trial (see Fig. 12B). None of the healthy control subjects showed hesitations during a turn.

Normative Study Results: Subjects' ages were not correlated with the turn angle estimates using the Merged Turn Algorithm (R=−0.15, p=0.09), unlike the El-Gohary et al. [1] (R=−0.18, p=0.04). Further, as expected, turn duration and number of steps per turn, were significantly correlated with age (R=0.45, p=1.8e-7; and R=0.34, p=8.4e-5). Table V provides the normative values for some of the turning measures with age.

V. DISCUSSION

In this study, we tested the generalizability of a turn algorithm using inertial sensors in several large cohorts that included different neurological cohorts across a large age range and with different protocols (total $n = 427$).

Our results demonstrate that our new, Merged Turn Algorithm correctly merges multiple small turns with short hesitations and results in turn angles closer to 180° across different cohorts for clinical tasks performed with a fixed turn angle (such as 180° turn during a 2-min walk test). In addition, our Discrete Turn Algorithm performed better in identifying sequential turns close in time compared to the El-Gohary algorithm [1], and showed a marginally improved agreement with the motion capture system.

Turning while walking is particularly challenging and more likely vulnerable to functional impairment than straight walking because turning involves more multisensory integration and coupling between posture and gait to maintain dynamic stability [35]. The challenge of turning can be reflected in hesitations, pauses, or stops during turns. These turn interruptions are quite common in elderly adults [36] and people with neurological disorders, such as freezing of gait in people with PD and balance corrections in people with ataxia. As a result of short pauses during 180° turns, any turn algorithm that is tested in healthy or neurological cohorts with a limited sample size may significantly underestimate turn angles (or amplitudes).

Turning, in fact, has been shown to be more sensitive than straight walking to early, mild PD, to freezing of gait in PD as well as to ataxia in people with multiple sclerosis [37], [38]. Quality of turning is also sensitive to fall risk in elderly people [39]. Turning quality measured from inertial sensors on the feet, ankles, or lumbar spine during normal daily activities has also been shown to be sensitive to PD [26], [40]. However, it is not clear if the smaller turn angles reported in people with PD than age-matched controls occur because people with PD voluntarily avoid large turns (example, to avoid freezing) or because they freeze or hesitate during large turns so large turns are measured as several smaller turns.

Merged Turn Algorithm. In addition to the improved estimates of turn angle closer to 180° compared to the El-Gohary algorithm [1], the Merged Turn Algorithm showed improved or similar results of turn angle estimates from recently published algorithms [8], [9], [12]. Specifically, the grouped average turn angle estimates were closer to 180°, and SD were reduced (see the summary table in Appendix for more details of reported turn angles in the literature).

As a result of consistent 180° turn angle estimation across different cohorts, the discriminative ability of turn duration and the number of steps required to complete a turn increased in both PD and SCA from their age-matched, healthy control groups. In fact, turn measures (such as turn duration and number of steps required to complete a turn) have been shown to better discriminate between neurological groups and healthy controls [3], [1], [15], [7].

As balance and gait impairments are affected by age, we also explored the effect of age on the turning characteristics in healthy control subjects and provided the normative data. Our findings are consistent with the findings of Thipgen [36], showing that the number of steps to complete the turn, and the total time required to complete a turn increased with age.

Discrete Turn Algorithm Walk-through doorway task has been shown to elicit freezing episodes in people with PD [41]. Hence, we designed a task mimicking the walking situation that arises during daily activities at home (for example, going from a common room to a kitchen) involving closely-spaced 180° and 90° turns, and our Discrete Turn Algorithm performed better in quantifying separate turns (not only 180° but also for a 90° turn) compared to the El-Gohary algorithm [1], and a reduction in the number of 270° turns (unwanted merge of 180° and 90° nearby turns). The results of walk-through doorways also provided an example in which adjacent turns shouldn't be merged. In addition, the Discrete Turn Algorithm showed an improved agreement with the motion capture system compared to El-Gohary et al. [1].

Important consideration for users.

The Merged Turn Algorithm can handle only one fixed turn angle as prior knowledge (such as 180° turns in the 2-minute walk task), but not a random variety of turn angles. The Merged Turn Algorithm also makes sure there is a sufficient period (>5 sec) between any turns in the same direction to ensure the algorithm does not merge turns that should be separated. So prior knowledge of turns includes: a) one fixed-angle turn and b) straight walking before and after turns. Note that the Merged Turn Algorithm could be easily modified to analyze other apriori sequences of turn angles. However, if a subject hesitates near the end of a turn, such that the Merged Turn Algorithm identifies two turns with turn angles of 160° and 20°, then it will not merge the second angle if it is <40° (minimum threshold required to detect a turn). Furthermore, if merging two turns results in a turn angle estimate to be further away from the fixed turn angle of 180°, then it will not merge nearby turns.

The algorithm described in this paper can be used for sensors at any location on the body. However, the start and end of a turn may be different depending on the sensor location. For

example the start of a turn may begin earlier and end later for sensors on the wrists or feet than on the trunk. The focus of our studies has been on characterizing turns near the center of mass, so we have only used sensors on the trunk, typically near the lumbar spine and sternum.

One of our long-term goals is to investigate turning impairments under unsupervised, passive conditions of daily life in which turn angle is not known. Thus, future work is needed to validate our Discrete Turning Algorithm in free-living conditions in people with and without neurological disorders.

VI. CONCLUSION

We evaluated two novel turn detection algorithms in several large cohorts that include different neurological disorders (total $n = 427$). We conclude that the Discrete Turn Algorithm is more accurate than the El-Gohary algorithm and is suitable for accurately detecting a sequence of turns of variable angles that occur close in time. We expect this will be especially suitable for characterizing turns during free-living conditions where a series of variable turns often occur close in time. We also conclude that the Merged Turn Algorithm is effective at detecting discrete turns with hesitations that are common to people with neurological disorders and combining these discrete turns into a single turn. This is appropriate for standard clinical evaluations such as the Timed Up and Go Test where the prescribed turn angles are known.

Supplementary Material

Refer to Web version on PubMed Central for supplementary material.

ACKNOWLEDGMENTS

This research was funded by the National Institutes of Health under award number R01AG006457 (PI: Horak), the Department of Veterans Affairs Merit Award number 5I01RX001075 (PI: Horak), and the Medical Research Foundation of Oregon (PI: Curtze). The authors thank all participants for generously donating their time to participate, Peter Fino, Mike Fleming, Heather Schlueter, Peter Martin, Graham Harker, and Hannah Casey for helping with data collection, and Daniel Peterson and Katrijn Smulders for data collection and help with study procedures.

REFERENCES

[1]. El-Gohary Met al., “Continuous monitoring of turning in patients with movement disability,” Sensors (Switzerland), vol. 14, no. 1, pp. 356–369, 2014, doi: 10.3390/S140100356.

[2]. Pham MHet al., “Algorithm for Turning Detection and Analysis Validated under Home-Like Conditions in Patients with Parkinson ’ s Disease and Older Adults using a 6 Degree-of-Freedom Inertial Measurement Unit at the Lower Back,” Front. Neurol, vol. 8, no. April, pp. 1–8, 2017, doi:10.3389/fneur.2017.00135. [PubMed: 28138322]

[3]. Salarian Aet al., “Analyzing 180 ° Turns Using an Inertial System Reveals Early Signs of Progression of Parkinson ’ s Disease,” pp. 224–227, 2009.

[4]. Mariani Bet al., “3D gait assessment in young and elderly subjects using foot-worn inertial sensors,” J. Biomech, vol. 43, pp. 2999–3006, 2010, doi: 10.1016/j.jbiomech.2010.07.003. [PubMed: 20656291]

[5]. Nutt JGet al., “Freezing of gait: moving forward on a mysterious clinical phenomenon,” Lancet Neurol, vol. 10, no. 8, pp. 734–744, 2011, doi: 10.1016/S1474-4422(11)70143-0. [PubMed: 21777828]

[6]. Beyea Jet al., “Convergent Validity of a Wearable Sensor System for Measuring Sub-Task Performance during the Timed,” Sensors (Basel), vol. 17, no. 934, pp. 1–18, 2017, doi: 10.3390/s17040934.

[7]. Bertoli Met al., “An Objective Assessment to Investigate the Impact of Turning Angle on Freezing of Gait in Parkinson ’ s Disease,” 2017 IEEE Biomed. Circuits Syst. Conf. (BioCAS), Turin, vol. 078492, pp. 0–3, 2017.

[8]. Haertner Let al., “Effect of Fear of Falling on Turning Performance in Parkinson ’ s Disease in the Lab and at Home Study Cohort Demographics and Clinical,” Front. aging Neurosci, vol. 10, no. 78, pp. 1–8, 2018, doi: 10.3389/fnagi.2018.00078. [PubMed: 29403371]

[9]. Meghji Met al., “An Algorithm for the Automatic Detection and Quantification of Athletes ’ Change of Direction Incidents Using IMU Sensor Data,” IEEE Sens. J, vol. PP, no. c, p. 1, 2019, doi: 10.1109/JSEN.2019.2898449.

[10]. Hsieh Cet al., “Automatic Subtask Segmentation Approach of the Timed Up and Go Test for Mobility Assessment System Using Wearable Sensors,” in 2019 IEEE EMBS International Conference on Biomedical & Health Informatics (BHI), 2019, pp. 1–4.

[11]. Ortega-bastidas Pet al., “Use of a Single Wireless IMU for the Segmentation the 3-m Timed Up & Go Test,” Sensors (Basel), vol. 19, no. 7, p. 1647, 2019, doi: 10.3390/s19071647.

[12]. Ur Rehman RZet al., “Turning Detection During Gait: Algorithm Validation and Influence of Sensor Location and Turning Characteristics in the Classification of Parkinson ’ s Disease,” Sensors (Basel, Switzerland)2, vol. 20, no. 5377, pp. 1–24, 2020.

[13]. Fleury Aet al., “A Fast Algorithm to Track Changes of Direction of a Person Using Magnetometers,” 2007 29th Annu. Int. Conf. IEEE Eng. Med. Biol. Soc. Lyon, pp. 2311–2314, 2007.

[14]. Yuji Het al., “Quantitative Evaluation of Movement Using the Timed Up-and-Go Test,” IEEE Eng. Med. Biol. Mag, vol. 27, no. 4, pp. 38–46, 2008. [PubMed: 18270049]

[15]. Weiss Aet al., “Using a Body-Fixed Sensor to Identify Subclinical Gait Difficulties in Older Adults with IADL Disability : Maximizing the Output of the Timed Up and Go,” PLoS One, vol. 8, no. 7, pp. 1–8, 2013, doi: 10.1371/journal.pone.0068885.

[16]. Mariani B and Jim C, “On-Shoe Wearable Sensors for Gait and Turning Assessment of Patients With Parkinson ’ s Disease,” IEEE Trans. Biomed. Eng, vol. 60, no. 1, pp. 155–158, 2013. [PubMed: 23268531]

[17]. Novak Det al., “Toward Real-Time Automated Detection of Turns during Gait Using Wearable Inertial Measurement Units,” Sensors (Basel), vol. 14, pp. 18800–18822, 2014, doi: 10.3390/s141018800. [PubMed: 25310470]

[18]. Nguyen HPet al., “Auto detection and segmentation of physical activities during a Timed-Up-and-Go (TUG) task in healthy older adults using multiple inertial sensors,” J. Neuroeng. Rehabil, vol. 12, no. 36, pp. 1–12, 2015, doi: 10.1186/s12984-015-0026-4. [PubMed: 25557982]

[19]. Fino PCet al., “Classifying Step and Spin Turns Using Wireless Gyroscopes and Implications for Fall Risk Assessments,” pp. 10676–10685, 2015, doi: 10.3390/s150510676.

[20]. Mariani Bet al., “On-shoe wearable sensors for gait and turning assessment of patients with parkinson’s disease,” IEEE Trans. Biomed. Eng, vol. 60, no. 1, pp. 155–158, 2013, doi: 10.1109/TBME.2012.2227317. [PubMed: 23268531]

[21]. Sabatini Angelo M., “Quaternion-based extended Kalman filter for determining orientation by inertial and magnetic sensing,” IEEE Trans. Biomed. Eng, vol. 53, no. 7, pp. 1346–1356, 2006. [PubMed: 16830938]

[22]. Fischer Cet al., “Tutorial: Implementing a pedestrian tracker using inertial sensors,” IEEE Pervasive Comput, vol. 12, no. 2, pp. 17–27, 2013, doi: 10.1109/MPRV.2012.16.

[23]. Epanechnikov VA, “Non-Parametric Estimation of a Multivariate Probability Density,” Theory Probab. Its Appl,vol. 14, no. 1, pp. 153–158, 1969, doi: 10.1137/1114019.

[24]. Fang Xet al., “Reference values of gait using APDM movement monitoring inertial sensor system,” R. Soc. open Sci, vol. 5, no. 1, p. 170818, 2018. [PubMed: 29410801]

[25]. Hollman JHet al., “Normative spatiotemporal gait parameters in older adults,” Gait Posture, vol. 34, no. 1, pp. 111–118, 2011, doi: 10.1016/j.gaitpost.2011.03.024. [PubMed: 21531139]

[26]. Mancini Met al., “Turn around freezing: Community-living turning behavior in people with Parkinson’s disease,” Front. Neurol, vol. 9, no. JAN, pp. 1–9, 2018, doi: 10.3389/fneur.2018.00018. [PubMed: 29403429]

[27]. Mancini Met al., “Mobility Lab to Assess Balance and Gait with Synchronized Body-worn Sensors,” J. Bioeng. Biomed. Sci, pp. 1–5, 2013, doi: 10.4172/2155-9538.s1-007.

[28]. Fino PCet al., “Inertial sensor-based centripetal acceleration as a correlate for lateral margin of stability during walking and turning,” IEEE Trans. Neural Syst. Rehabil. Eng, [Online]. Available: doi: 10.1109/TNSRE.2020.2971905.

[29]. Zatsiorsky VM and Seluyanov VN, “The mass and inertia characteristics of the main segments of the human body,” Biomech. VIII-B, Nayoga, Jpn, vol. 4-B, pp. 1152–1159, 1983.

[30]. King LAet al., “Do cognitive measures and brain circuitry predict outcomes of exercise in Parkinson Disease : a randomized clinical trial,” BMC Neurol, pp. 4–11, 2015, doi: 10.1186/s12883-015-0474-2. [PubMed: 25648431]

[31]. Nieuwboer Aet al., “Reliability of the new freezing of gait questionnaire : Agreement between patients with Parkinson ’ s disease and their carers,” Gait Posture, vol. 30, pp. 459–463, 2009, doi: 10.1016/j.gaitpost.2009.07.108. [PubMed: 19660949]

[32]. Bland JM and Altman DG, “Statistical methods for assessing agreement between two methods of clinical measurement,” Lancet, vol. 327, no. 8476, pp. 307–310, 1986.

[33]. Shrout PE and Fleiss JL, “Intraclass Correlations : Uses in Assessing Rater Reliability,” Psychol. Bull, vol. 86, no. 2, pp. 420–428, 1979. [PubMed: 18839484]

[34]. Turck Net al., “pROC: an open-source package for R and S+ to analyze and compare ROC curves,” BMC Bioinformatics, vol. 8, pp. 12–77, 2011, doi: 10.1007/s00134-009-1641-y.

[35]. Horak FB and Mancini M, “Objective bio markers of balance and gait for Parkinson’s disease using body-worn sensors,” Mov. Disord, vol. 28, no. 11, pp. 1544–1551, 2013, doi: 10.1002/mds.25684. [PubMed: 24132842]

[36]. Thigpen MT, “Turning Difficulty Characteristics of Adults Aged 65 Years or Older,” Phys. Ther, vol. 80, no. 12, pp. 1174–1187, 2000, doi: 10.1093/ptj/80.12.1174. [PubMed: 11087304]

[37]. Zampieri Cet al., “The instrumented timed up and go test: Potential outcome measure for disease modifying therapies in Parkinson’s disease,” J. Neurol. Neurosurg. Psychiatry, vol. 81, no. 2, pp. 171–176, 2010, doi: 10.1136/jnnp.2009.173740. [PubMed: 19726406]

[38]. Spain RIet al., “Body-worn motion sensors detect balance and gait deficits in people with multiple sclerosis who have normal walking speed,” Gait Posture, vol. 35, no. 4, pp. 573–578, 2012, doi: 10.1016/j.gaitpost.2011.11.026. [PubMed: 22277368]

[39]. Mancini Met al., “Continuous Monitoring of Turning Mobility and Its Association to Falls and Cognitive Function: A Pilot Study,” vol. 71, no. 8, pp. 1102–1108, 2016, doi: 10.1093/gerona/glw019.

[40]. Shah VVet al., “Quantity and quality of gait and turning in people with multiple sclerosis, Parkinson ’ s disease and matched controls during daily living,” J. Neurol, vol. 267, no. 4e, pp. 1188–1196, 2020, doi: 10.1007/s00415-020-09696-5. [PubMed: 31927614]

[41]. Cowie Det al., “Doorway-provoked freezing of gait in Parkinson’s disease,” Mov. Disord, vol. 27, no. 4, pp. 492–499, 2012, doi: 10.1002/mds.23990. [PubMed: 21997389]

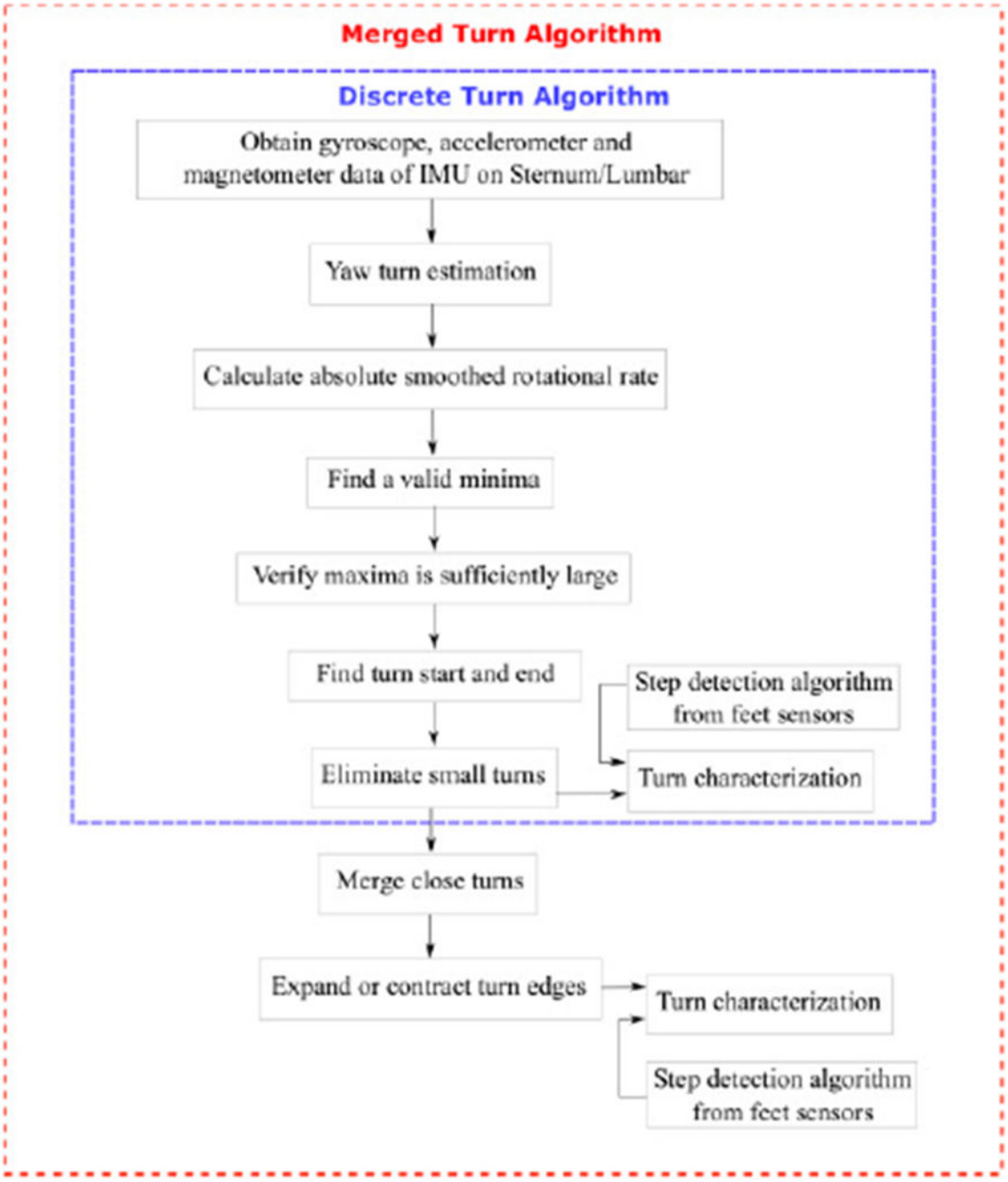

Fig. 1.
Flowchart of the proposed turning algorithms.

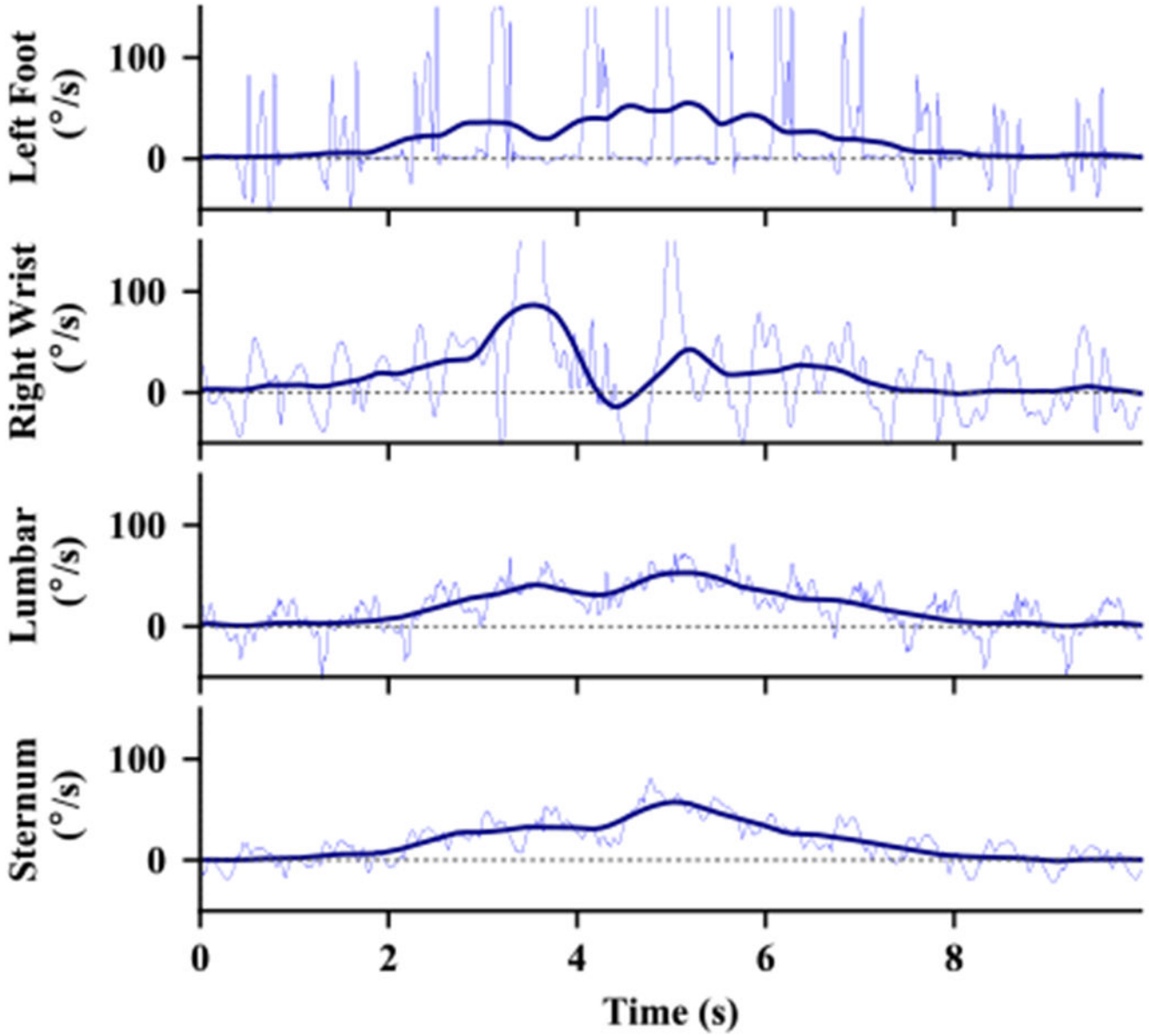

Fig. 2.

Example of the vertical rotational rate during a 180° turn from sensors at different locations. The thin, blue lines show the original angular velocity signal and the thick, dark lines show the signal after smoothing with the filter.

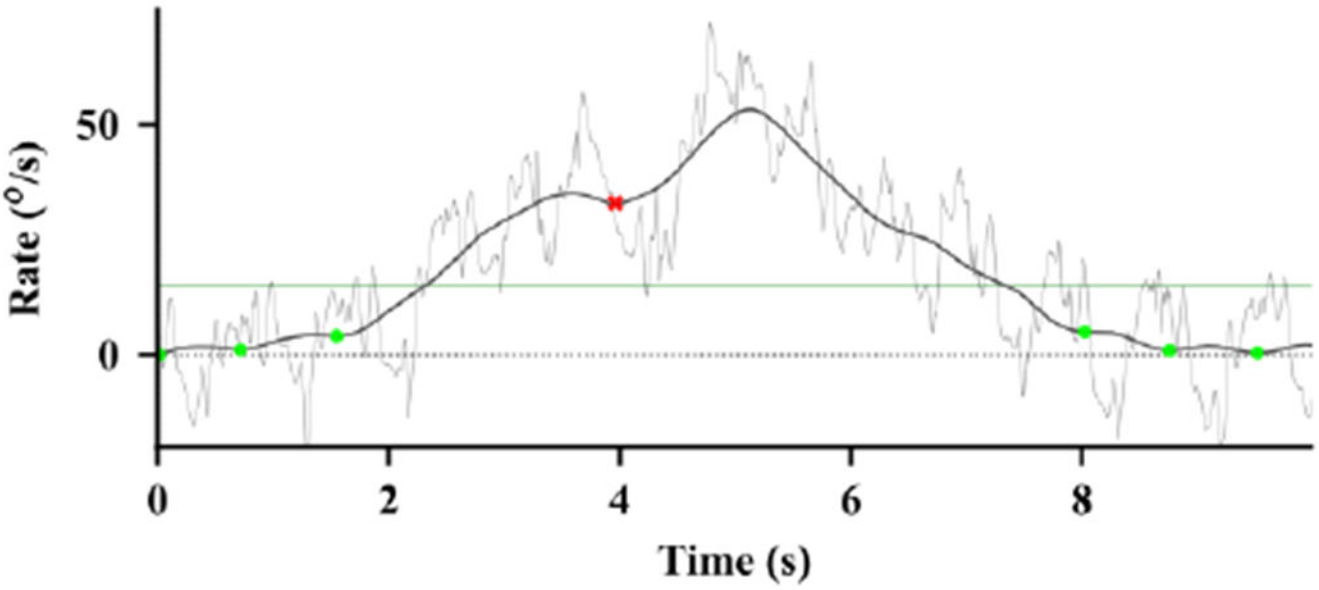

Fig. 3.

Example of the detection of minima before and after a turn. The thin light line shows the vertical rotational rate. The thick, dark line shows the absolute value of the smoothed vertical rotational rate. The dots show valid minima, and the red x shows a minimum that was too shallow and was declared as invalid. The thin horizontal line shows the threshold for detection (ν_d) between minima.

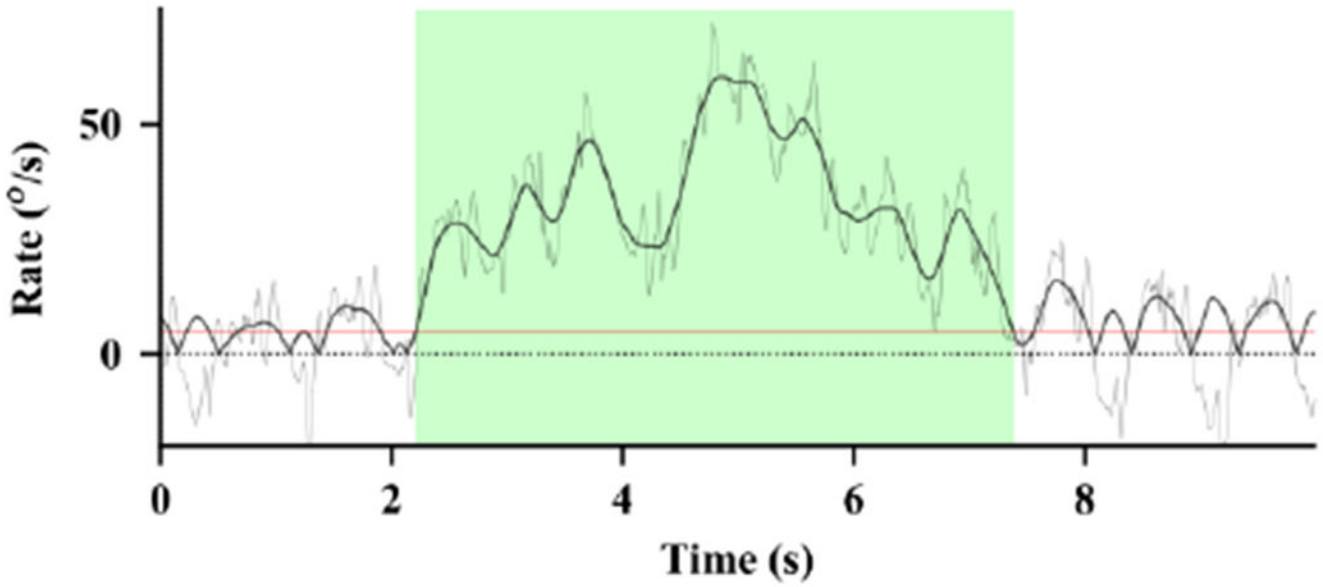

Fig. 4.

Example of the detection of edges demarcating the start and end of a turn. The thin, light line shows the vertical rotational rate. The thick black line shows the absolute value of the signal after smoothing with the edge filter. The horizontal red line shows a detection threshold for edges (v_e). The detected turn, including the beginning and end of the turn, is shown by the green shaded region.

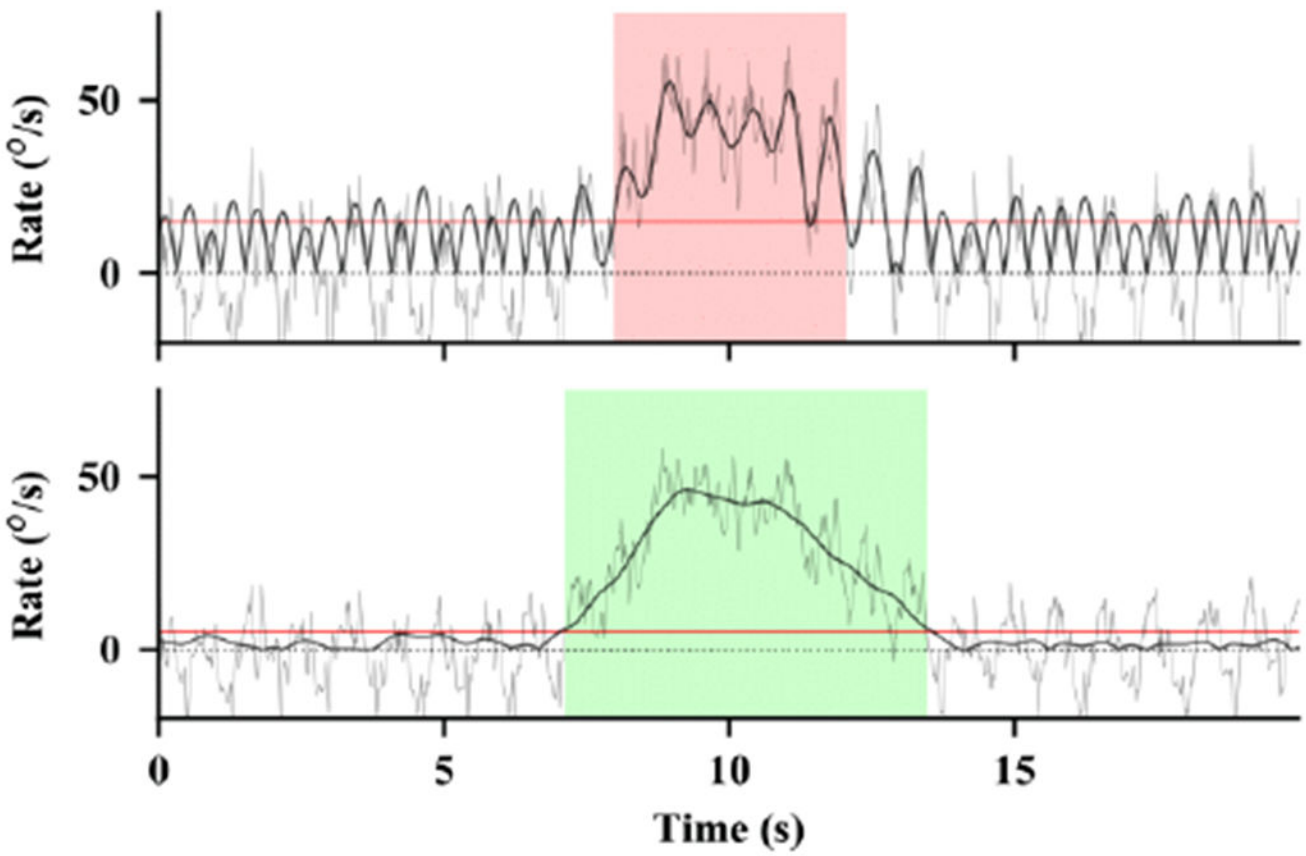

Fig. 5.

Example of a turn detection algorithm by El-Gohary et al. [1] (top) compared to the proposed Discrete Turn Algorithm (bottom). Both figures show different estimates of the vertical rotational rate of the same recording.

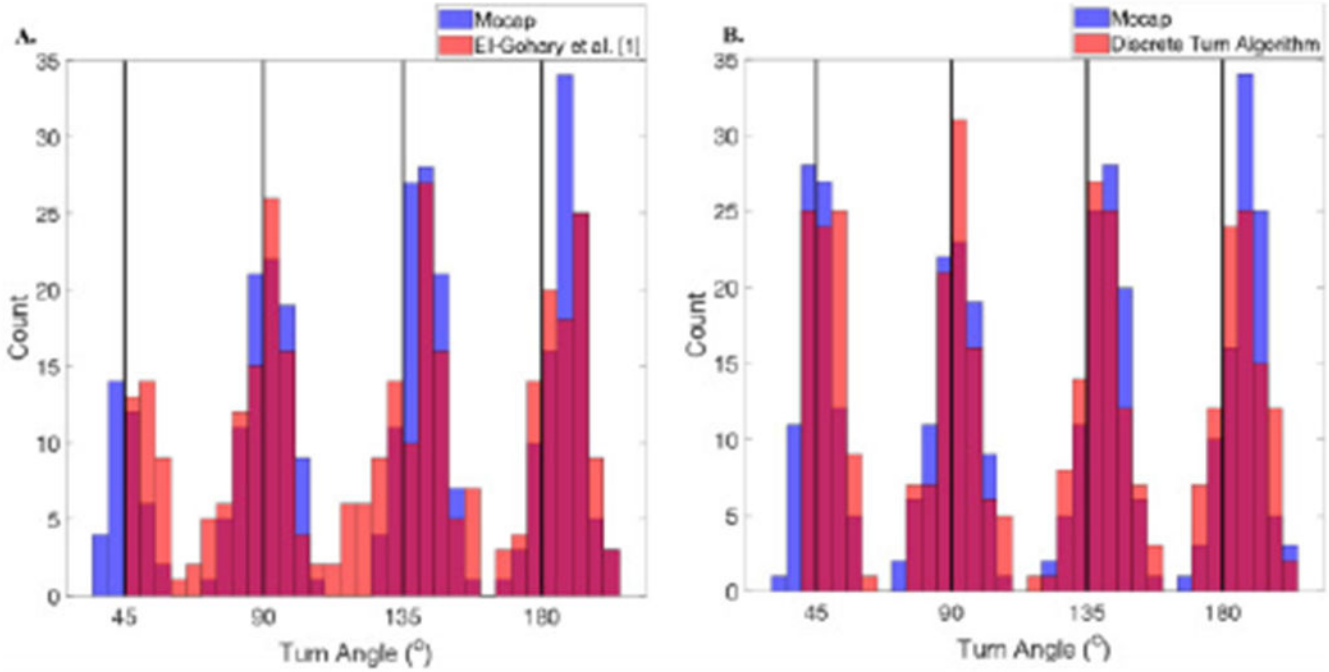

Fig. 6.

Histogram of turn angle estimates comparing A) El-Gohary et al. [1] algorithm to the optical motion capture, and B) the Discrete Turn Algorithm to the optical motion capture on the validation dataset.

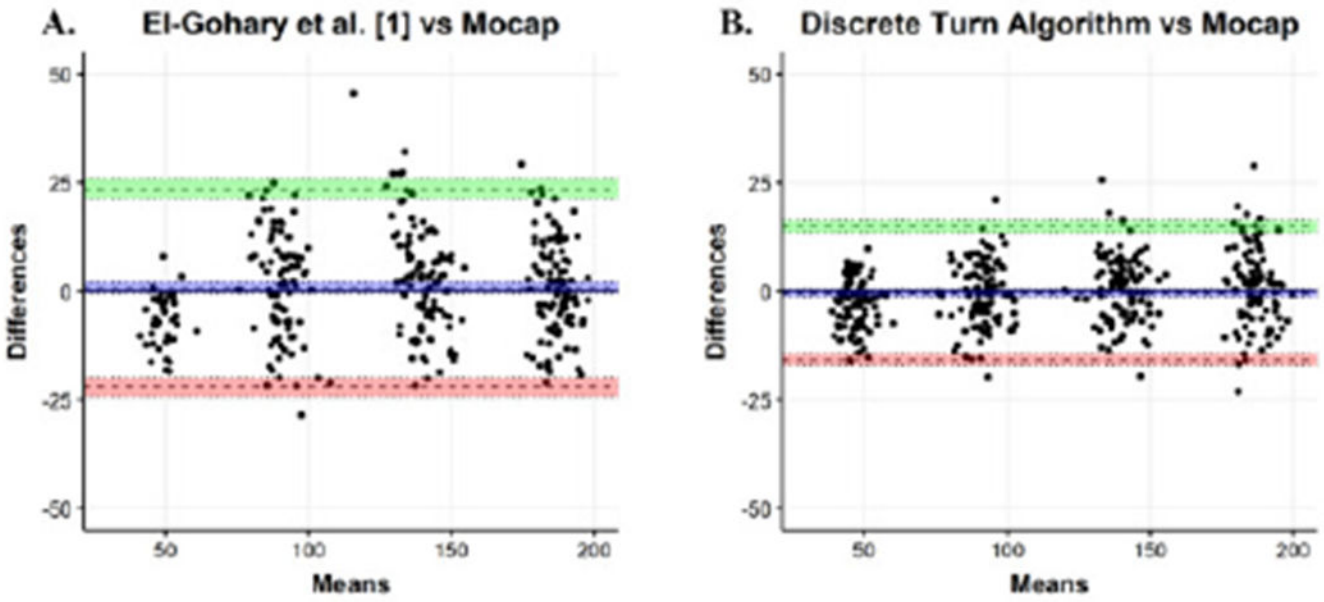

Fig. 7.

Bland Altman plot for agreement between the turn angle estimates using A) optical motion capture and El-Gohary et al. [1], and B) the Discrete Turn Algorithm for the Validation Study.

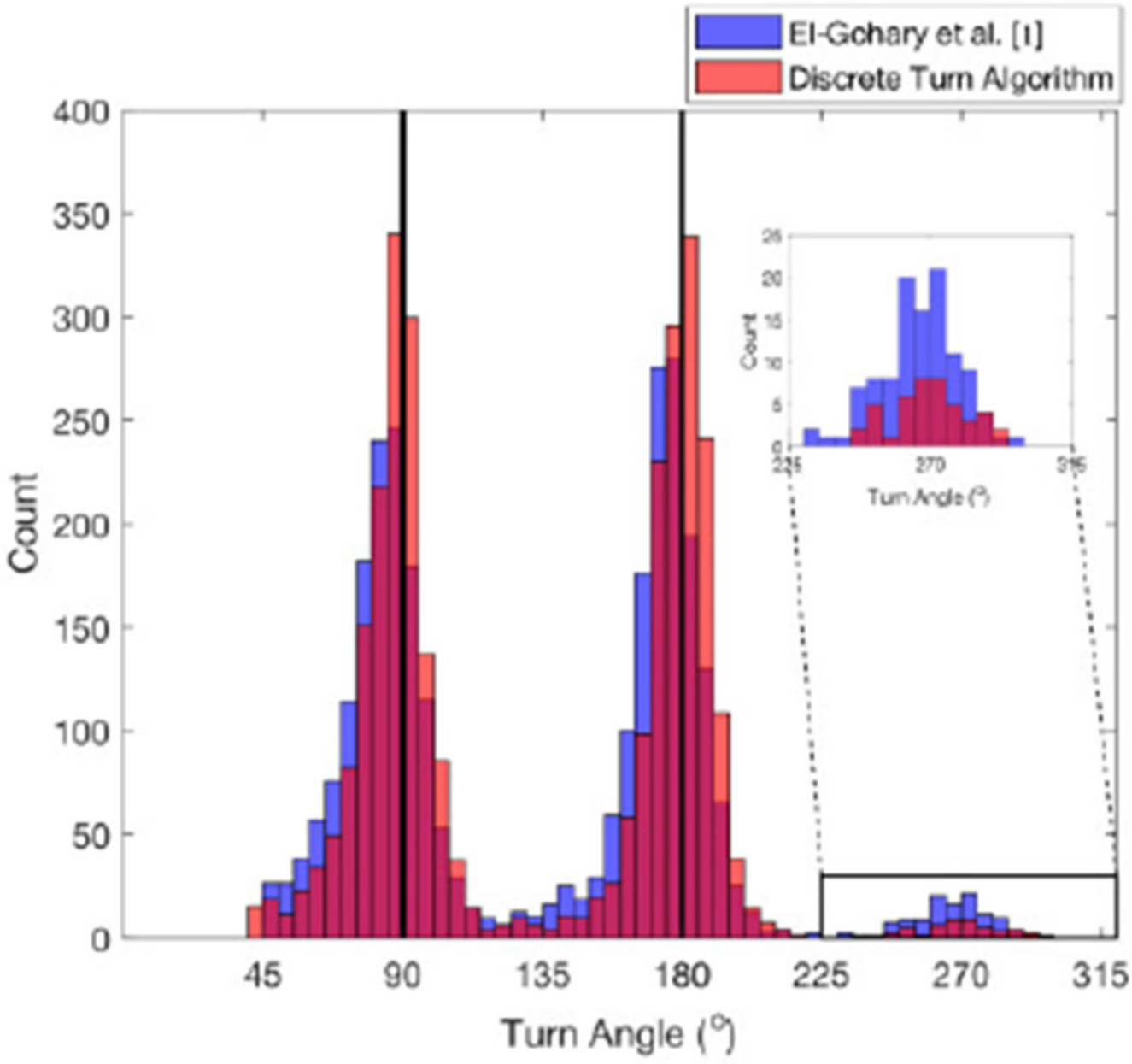

Fig. 8.

Histogram of turn angle estimates comparing El-Gohary et al. algorithm [1] and the Discrete Turn Algorithm for walk-through doorway dataset.

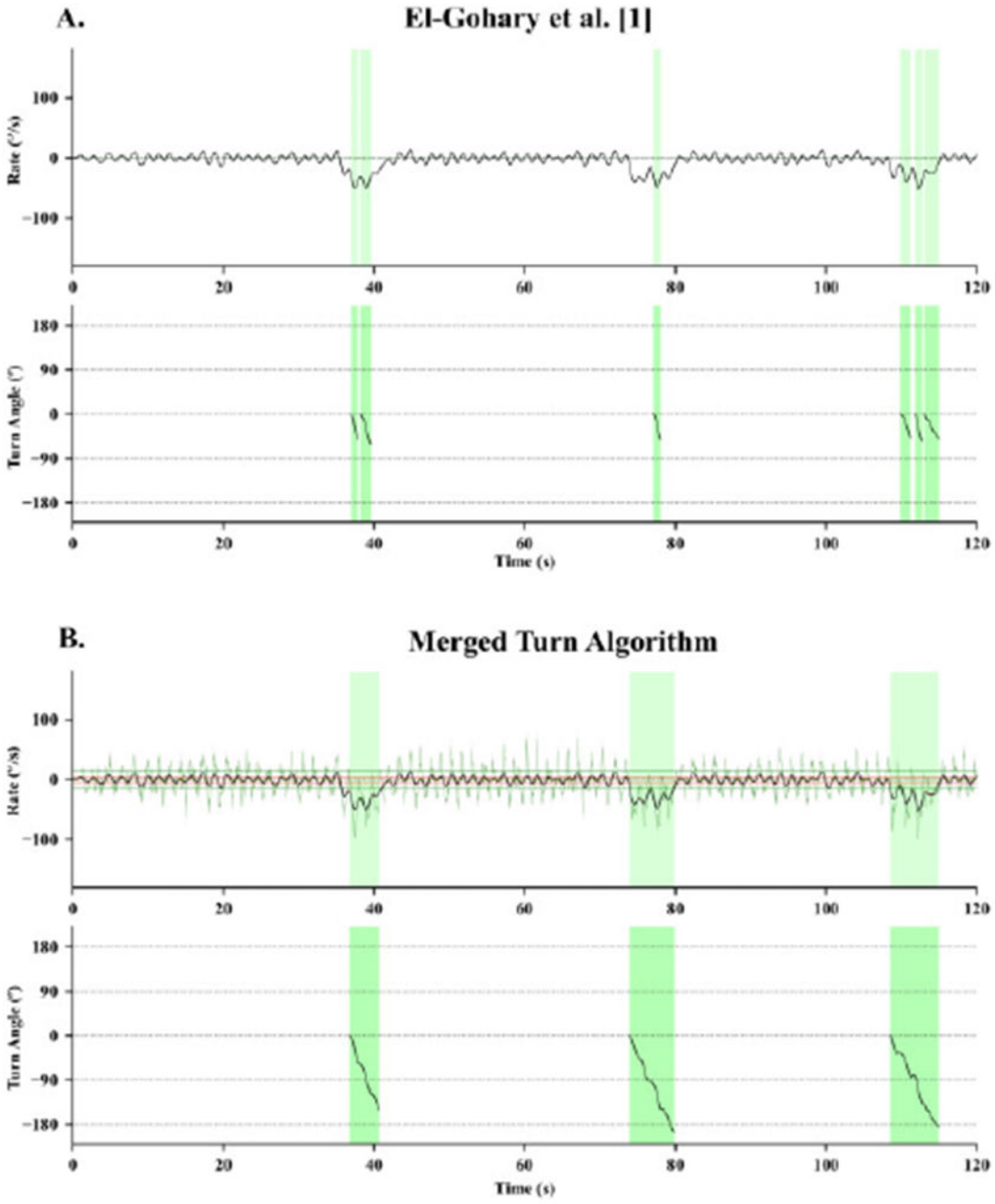

Fig. 9.

An example of the performance of three turn angle estimates during a 2-minute walk test, using A) El-Gohary et al. [1] and B) the Merged Turn Algorithm in a severe patient with SCA. The top graph shows the yaw gyroscope signal, and the bottom graph shows the turn angle measure form each algorithm. Green areas show the start and end of each turn, as detected by the two algorithms.

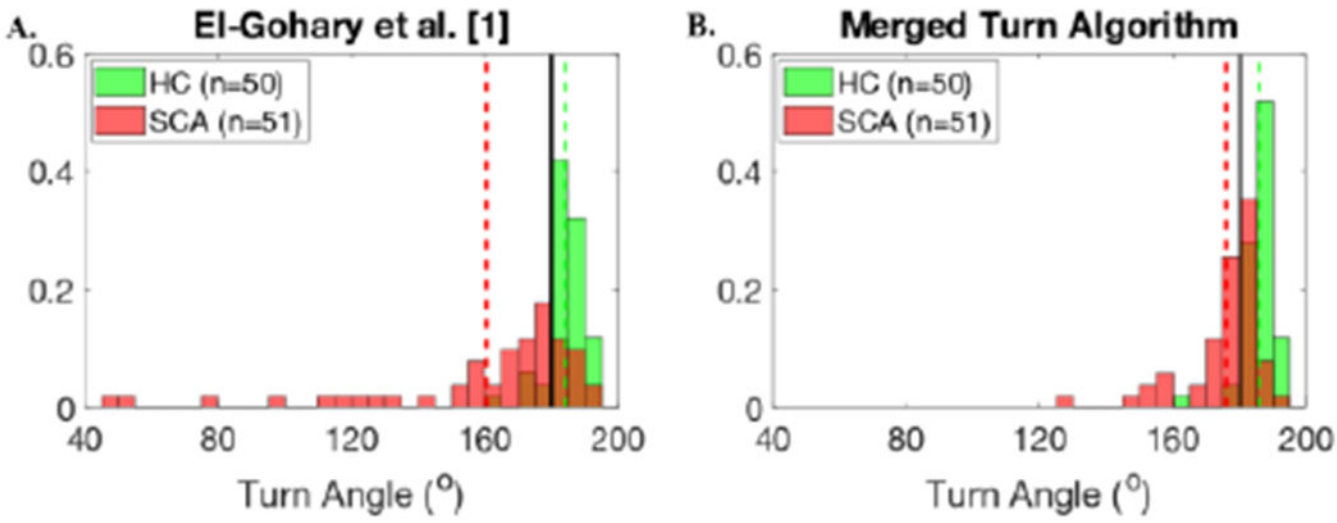

Fig. 10.

Histogram of turn angle estimates using A) El-Gohary et al. [1], and B) the Merged Turn Algorithm for PD/HC dataset. Subjects with PD and FOG show smaller turns due to hesitations than PD without FOG (nFOG) or HC.

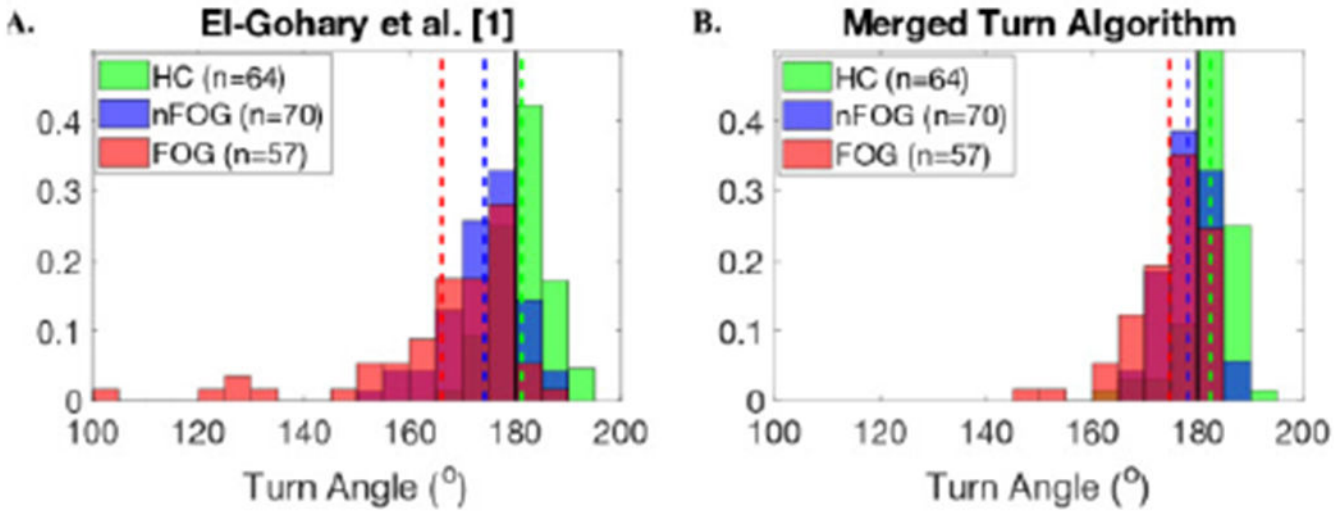

Fig. 11.

Histogram of turn angle estimates using A) El-Gohary et al. [1], and B) the Merged Turn Algorithm for SCA/HC dataset.

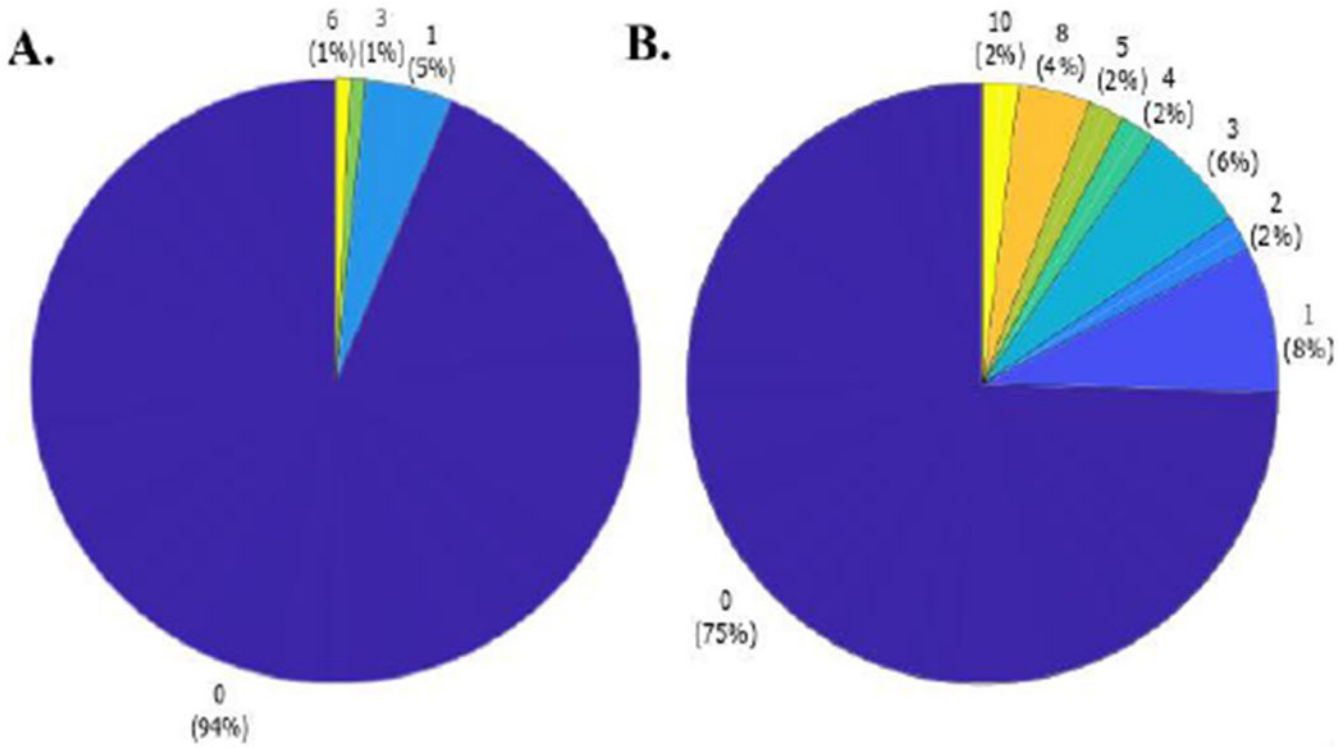

Fig. 12.
Pie chart of the number of hesitations per trial in A) people with PD, and B) SCA.

TABLE I

DESIGN PARAMETER VALUES FOR THE DISCRETE AND MERGED TURN ALGORITHM

Symbol	Description	Value
d_d	Detection filter impulse response duration	1.476 s
d_e	Edge filter impulse response duration	0.383 s
η	Required depth for minima	10.0 °/s
ν_d	Required velocity peak to detect turn	15.0 °/s
ν_e	Required velocity peak to detect turn edges	5.0 °/s
θ	Required turn angle to be detected	40.0 °
t_s	Maximum turn separation interval for merge	5.0 s
ν_x	Required velocity peak to detect edge	2.5 °/s
ν_c	Required velocity peak to detect edge	7.5°/s

TABLE II

SUMMARY OF OUR STUDIES AND PROTOCOLS USED TO TEST THE PERFORMANCE OF THE PROPOSED ALGORITHMS WITH SENSORS WERE PLACED ON STERNUM AND LUMBAR AREAS.

Study	Number of Subjects	Protocol	Expected Turn Angle	Turn Metrics Used
Discrete Turn Algorithm				
Development dataset				
Validation (HC)	HC: n = 10 (age: 72 ± 5.8 years)	Predefined turning angles	45° 90° 135° 180°	Turn angle (°)
Test dataset				
Walk-through doorway (PD/HC)	PD: n = 127 (age: 69.20 ± 7.71 years) HC: n = 64 (age: 67.36 ± 8.21 years)	Walk-through doorway	180° 90°	Turn angle (°)
Merged Turn Algorithm				
Development dataset				
PD/HC	PD: n = 127 (age: 69.20 ± 7.71 years) HC: n = 64 (age: 67.36 ± 8.21 years)	2-min walk test	180°	Turn angle (°) Turn Duration (s) Steps in Turn (#) Turn Rate Average (°/s) Turn Rate Max (°/s) Turn Hesitations (#)
SCA/HC	SCA: n = 51 (age: 54.51 ± 13.31 years) HC: n = 50 (age: 55.78 ± 14.77 years)	2-min walk test	180°	Turn angle (°) Turn Duration (s) Steps in Turn (#) Turn Rate Average (°/s) Turn Rate Max (°/s) Turn Hesitations (#)
Test dataset				
Normative (HC)	HC: n = 125 (age range: 19 – 88 years)	400 m fast walk with cone	180°	Turn angle (°) Turn Duration (s) Steps in Turn (#) Turn Rate Average (°/s) Turn Rate Max (°/s) Turn Hesitations (#)

TABLE III

COMPARISON OF PERFORMANCE OF THE PROPOSED ALGORITHMS WITH EL-GOHARY ET AL. [1] FOR VARIOUS TURNING METRICS (MEAN ± SD) IN DISCRIMINATING PD FROM HC DURING 180° TURNS IN A PRESCRIBED 2-MINUTE WALK.

Metric	El-Gohary et al. [1]			Discrete Turn Algorithm			Merged Turn Algorithm		
	HC (N=64)	PD (N=127)	AUC	HC (N=64)	PD (N=127)	AUC	HC (N=64)	PD (N=127)	AUC
Turn Angle (°)	181.17 ± 5.19	170.51 ± 12.72	**0.84**	183.68 ± 5.24	175.52 ± 11.31	**0.83**	182.40 ± 4.88	176.63 ± 6.42	**0.82**
Turn Duration (s)	2.08 ± 0.26	2.63 ± 0.49	**0.87**	2.46 ± 0.26	3.19 ± 0.67	**0.90**	2.41 ± 0.26	3.26 ± 0.96	**0.91**
Steps in Turn (#)	3.42 ± 0.71	4.36 ± 1.00	**0.80**	4.28 ± 0.60	5.49 ± 1.13	**0.85**	4.16 ± 0.57	5.56 ± 1.54	**0.87**
Turn Rate Average (°/s)	89.29 ± 11.55	67.71 ± 13.99	**0.90**	76.16 ± 8.50	57.5 ± 11.50	**0.92**	77.29 ± 8.57	57.95 ± 11.97	**0.92**
Turn Rate Max (°/s)	191.49 ± 27.76	138.48 ± 34.83	**0.89**	181.19 ± 25.71	132.61 ± 33.29	**0.88**	181.19 ± 25.71	132.90 ± 33.00	**0.88**

TABLE IV

COMPARISON OF PERFORMANCE OF THE PROPOSED ALGORITHMS WITH EL-GOHARY ET AL. [1] FOR VARIOUS TURNING METRICS (MEAN ± SD) IN DISCRIMINATING SCA FROM HC DURING 180° TURNS IN A PRESCRIBED 2-MINUTE WALK.

Metric	El-Gohary et al. [1]			Discrete Turn Algorithm			Merged Turn Algorithm		
	HC (N=50)	SCA (N=51)	AUC	HC (N=50)	SCA (N=51)	AUC	HC (N=50)	SCA (N=51)	AUC
Turn Angle (°)	184.3 ± 6.48	160.52 ± 33.14	**0.84**	187.16 ± 7.93	166.14 ± 31.67	**0.88**	185.93 ± 5.21	175.99 ± 11.87	**0.86**
Turn Duration (s)	2.10 ± 0.28	2.50 ± 0.52	**0.76**	2.48 ± 0.34	2.98 ± 0.60	**0.77**	2.43 ± 0.35	3.61 ± 1.42	**0.86**
Steps in Turn (#)	3.60 ± 0.81	4.16 ± 1.25	**0.68**	4.52 ± 0.61	5.18 ± 1.18	**0.74**	4.39 ± 0.63	5.98 ± 1.59	**0.87**
Turn Rate Average (°/s)	90.45 ± 13.48	66.48 ± 16.47	**0.87**	77.47 ± 10.91	57.60 ± 14.05	**0.87**	78.98 ± 10.95	55.87 ± 16.48	**0.89**
Turn Rate Max (°/s)	201.63 ± 41.18	151.14 ± 41.11	**0.81**	186.77 ± 37.18	137.07 ± 36.77	**0.83**	187.07 ± 37.17	138.36 ± 35.53	**0.83**

TABLE V

MEAN AND SD OF TURN METRICS USING THE MERGED TURN ALGORITHM FOR NORMATIVE DATA.

Metric	≥19 and <45 (n = 28)	≥45 and <65 Years (n = 46)	≥65 (n = 51)
Turn Angle (°)	183.61 ± 4.30	185.23 ± 5.69	181.57 ± 5.94
Turn Duration (s)	2.17 ± 0.21	2.30 ± 0.28	2.56 ± 0.45
Steps in Turn (#)	4.64 ± 0.55	4.98 ± 0.65	5.23 ± 0.79
Turn Rate Average (°/s)	85.73 ± 8.42	82.44 ± 11.25	73.68 ± 12.73
Turn Rate Max (°/s)	226.68 ± 31.61	215.43 ± 40.88	189.40 ± 44.10